Cellulose (2019) 26:5757–5768
https://doi.org/10.1007/s10570-019-02455-4

ORIGINAL RESEARCH

Rational design of cotton substrates with enhanced UV–blocking, high antibacterial efficiency and prominent hydrophobicity

Wei Ma · Lin Li · Xuehong Ren · Tung-Shi Huang

Received: 9 March 2019 / Accepted: 23 April 2019 / Published online: 27 April 2019

Abstract In this study, cotton fabrics with improved antibacterial efficiency and hydrophobic properties were prepared with the coatings of N-halamine siloxanes, ZnO, and silane precursors by the ultrasonic-assisted dipping-padding assembly technique. The coated cotton fabrics were characterized by FT-IR, SEM, XRD and XPS. The chlorinated cotton fabrics showed good hydrophobicity with water contact angle of $139^{o} \pm 2^{o}$. With the addition of ZnO in the N-halamine coatings, the chlorinated samples showed good antibacterial efficacy and could inactivate both all inoculated *Escherichia coli* O157:H7 (ATCC 43895) and *Staphylococcus aureus* (ATCC 6538) within 10 min. The chlorinated samples also showed good viability to mammalian cells. The stabilities of the coated cotton towards UV light and washing cycles and mechanical properties were investigated. Over 69% of the chlorine was retained after the equivalent of 25 machine washes. The N-halamine siloxanes coating of cotton with ZnO nanoparticles significantly enhanced the UV stability. In addition, the coated cotton fabrics maintained high tensile strength and fair air permeability.

W. Ma · L. Li · X. Ren (✉)
College of Textiles and Clothing, Jiangnan University, Wuxi 214122, Jiangnan, China
e-mail: xhren@jiangnan.edu.cn

T.-S. Huang
Department of Poultry Science, Auburn University, Auburn, AL 36849, USA

Graphical abstract

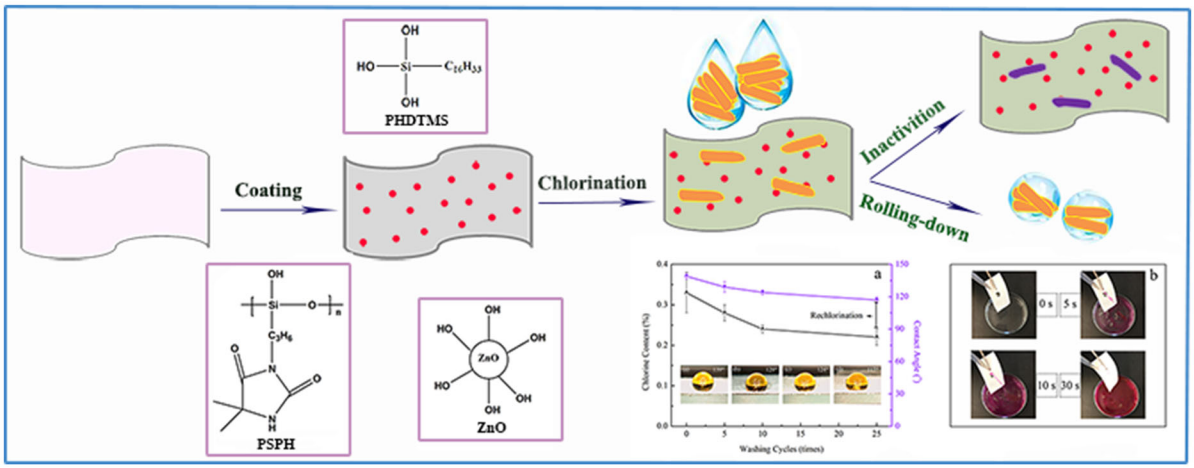

Keywords N-halamine · ZnO · Cotton · Hydrophobic · Antibacterial · UV light stability

Introduction

The development of new antimicrobial materials in textile helps in the reduction of harmful bacteria. Cellulose, an excellent natural material, could be considered as the major inexhaustible source of raw materials, and meets the increasing appeal for green and biocompatible products. However, textiles made from cellulose are easily contaminated with bacteria and other pathogenic microorganisms under an appropriate environments, such as suitable temperatures and humidity, etc.(Shahidi et al. 2017; Xu et al. 2017; Yazhini and Prabu 2015). Thus, cellulosic materials with antibacterial abilities and hydrophobic properties are highly desirable.

Of the various antibacterial materials, metal oxides and metal ions, N-halamines, and quaternary ammonium salts have attracted significant research interest. N-halamines, as predominant biocides, have drawn great attention over others for their antimicrobial efficacy against a broad-spectrum of microorganisms, long-term stabilities and regenerabilities (Demir et al. 2017; Dong et al. 2015). Recently, nanosized N-halamines have also been investigated due to their enhanced antibacterial efficiency. Jang et al. (2008), Yu et al. (2013) and Zhao et al. (2014)) investigated the effect of particle size of hydantoin/SiO_2 on antibacterial activity and their results showed that small particles had more functional N-halamine sites on the surface leading on enhanced antibacterial efficiency. Dong et al. (2014) prepared N-halamine-decorated polystyrene nanoparticles to study the correlation of antibacterial activity with surface area using a plate counting test and confirmed that the smaller particles had higher antibacterial activity. However, under UV irradiation, N–Cl bonds and bonds between N-halamine and substrates decompose rapidly, leading to the loss of antimicrobial activity (Kocer et al. 2010).

Several metal oxides such as ZnO, TiO_2, MgO and CaO exhibit high photocatalytic properties and could be used as UV absorbers, self-cleaning materials, and photo-sensors, etc. (Chen et al. 2015; Dong et al. 2016; Horsthuis 2017; Jin et al. 2014), increasing their popularity in recent research. Among these compounds, ZnO has been considered as one of the most promising photocatalysts due to its wide band gap energy (3.37 eV), availability, low cost, physical and chemical stability, and high oxidative capacity (Olson et al. 2015; Silva et al. 2017; Zhang et al. 2016a). Up to now, few studies have been reported to hybridize N-halamine with ZnO nanoparticles.

Hydrophobic coatings combined with different substrates have been reported to improve antibacterial abilities of textiles by rolling droplets to remove bacteria, which has certain guiding significance to the development of outdoor sportswear via forming self-

cleaning surface (Jeong et al. 2016; Zhang et al. 2016b). Herein, in this work, we modified cotton fabric with composites produced from N-halamine precursors, ZnO, and hexadecyltrimethoxysilane via a simple pad-dry-cure process (Scheme 1). The coated cotton fabrics were characterized by FT-IR, SEM, XRD and XPS. Intrinsic hydrophobic character was identified by contact angle and sliding angle measurements after different washing cycles. Antimicrobial behaviors of composites were investigated against both *Escherichia coli* O157:H7 (*E. coli* O157:H7) and *Staphylococcus aureus* (*S. aureus*) strains. In addition, UV light stability, UPF value, ventilation properties and in vitro cytocompatibility were studied.

Experimental section

Materials and instruments

A 100% bleached cotton fabric was purchased from Zhejiang Guangong Printing & Dyeing Company, China. 5,5-Dimethylhydantoin was provided by Hebei Yaguang Fine Chemical Co., Ltd. Hexadecyltrimethoxysilane (HDTMS) and γ-chloropropyltriethoxysilane were supplied by J&K Scientific Ltd, Shanghai, China. Other chemical reagents in this research were purchased from Sinopharm Chemical Reagent Co., Ltd. All reagents were used as received without further purification.

Fourier transform infrared (FT-IR) spectra were obtained to confirm the chemical composition of the modified fabric surfaces using a NEXUS 470 spectrometer (Nicolet Instrument Corporation, USA). An ESCALAB 250 Xi (Thermo Scientific, USA) was used to detect X-ray photoelectron spectroscopy (XPS) of the modified cotton. X-ray diffractometer (Bruke AXS, Germany) was used to characterize the crystal structure of the samples in a 2θ range of 10°–80°. Scanning electron microscope (SU-1510, Japan) was used to visualize the morphology and distribution.

Synthesis of ZnO NPs

Briefly, zinc acetate dehydrate (60 mmol) was dissolved in 40 mL methanol, and 60 mL of methanol solution containing potassium hydroxide (130 mmol) was added drop wise into the above solution. After refluxing at 60 °C for 72 h, the product of ZnO NPs was washed with ethanol for five times, isolated by centrifugation (10,000 rpm), and dried in an oven at 50 °C.

Cotton fabric modified with N-halamine, ZnO, and hexadecyltrimethoxysilane

Poly[5,5-dimethyl-3-(3′-triethoxysilylpropyl)-hydantoin] (PSPH) was synthesized according to the method reported previously(Worley et al. 2005) and the structure was shown in Scheme 1. Typically, a bath containing 5% PSPH and 5% ZnO in a 1:1 by weight of ethanol and water was prepared. Swatches of 100% cotton fabric were soaked in the bath with sonication for 30 min, and dried at 95 °C for 5 min. HDTMS

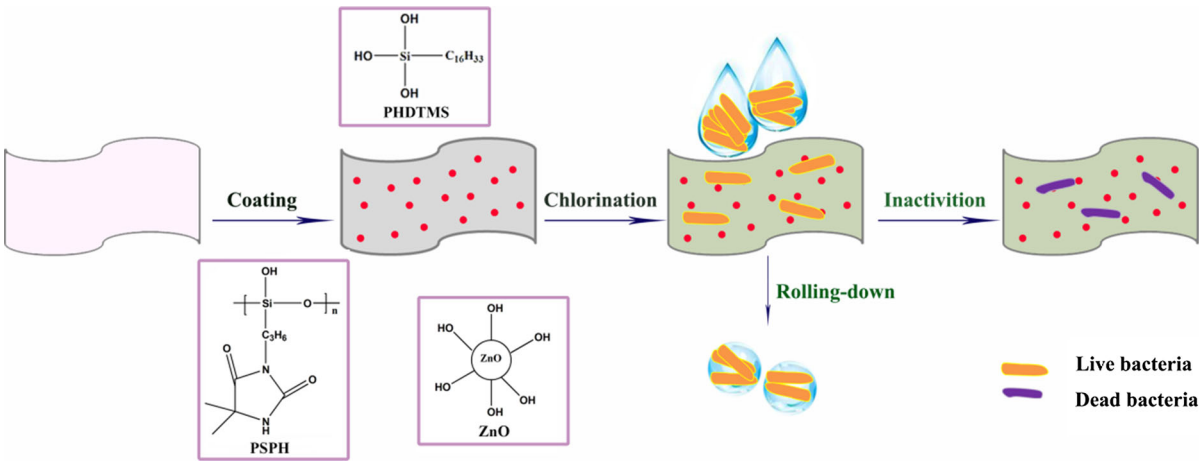

Scheme 1 Schematic illustration of the preparation of antibacterial and hydrophobic cotton fabric

(5 g) in another flask was completely hydrolyzed in acetate for 30 min. The above swatches were immersed in the complexes for 15 min with sonication, padded through a laboratory wringer, dried at 95 °C for 1 min, and cured at 130 °C for 3 min. The treated cotton swatches (labeled as PSPH–ZnO–PHDTMS/cotton) were soaked in a 0.5% detergent solution for 15 min to remove un-reacted agents, rinsed several times with distilled water, and dried at room temperature.

Chlorination and titration

A 10% commercial aqueous sodium hypochlorite (NaClO) was selected as the reagent to provide oxidizing chlorine. The treated swatches were soaked in NaClO solution at pH 7 for 2 h. After the chlorination, the samples were washed thoroughly with distilled water and dried for 60 min at 45 °C to remove unbound chlorine. The loaded chlorine concentrations on the samples were determined by iodometric/thiosulfate titration method. The weight percentage of oxidative Cl^+ of the samples was calculated using the following Eq. 1.

$$Cl^+(\%) = \frac{N \times V \times 35.45}{2 \times W} \times 100 \quad (1)$$

where N and V are the normality (equiv/L) and volume (L) of sodium thiosulfate, respectively, and W is the weight (g) of tested sample.

Washing stability and hydrophobicity tests

The accelerated washing test was performed by a standard procedure according to AATCC 61-1996 Test Method. The treated samples (2.54 × 5.08 cm^2) were put into stainless steel canisters with 50 stainless steel balls and 150 mL detergent water solution, and washed at 42 rpm and at 49 °C for 45 min. One washing cycle is equivalent to 5 commercial launderings. After certain washing cycles, the samples were rinsed using distilled water and dried. The chlorine contents remaining on the samples were determined according to Eq. 1. The water contact angle and water sliding angle of the treated cotton fabrics were measured by the digital microscope contact angle tester (26700-300, Instrument & Equipment Specialties Inc. USA). Drops of dyed water (0.2 mg/mL methyl orange, 10 μL) were added on the fabric surface and after 1 min, the contact angle was measured. Meanwhile, sliding angle of 15 μL water was measured with above equipment with the clockwise rotation rate at 2°/s. The average of the five measurements was used for analysis. Furthermore, in order to evaluate its self-cleaning performance directly after washing cycles, a stream of water was used to remove contamination (Rhodamine B, 2 mg) from the surface of fabrics.

Measurement of mechanical properties

According to the GB/T3923-1998 method, the breaking strengths of the samples were measured using an electronic fabric strength tester (YG(B)461E, China). Fabrics were cut into 50 × 200 mm^2 pieces, and 5 pieces of each sample were measured. All of the samples were stored and tested under the controlled environmental conditions.

UV light stability, UPF value and ventilation property test

UV light stability of Cl–PSPH–PHDTMS/cotton and Cl–PSPH–ZnO–PHDTMS/cotton were performed on an Accelerated Weathering Tester conforming to the ASTMD4587 standards. Each specimen with dimension of 2 × 2 cm^2 was exposed horizontally to 0.89 W/m^2 external heat flux (Type A, 315–400 nm, 60 °C). The samples were removed from the UV chamber and titrated, or rechlorinated and titrated after exposure to UV light with times in the range of 1 h to 72 h.

According to AS/NZ 4399:1996, the UV-protection level of fabrics can be rated into three levels based on the UPF values: good (UPF = 15–24), very good (UPF = 25–39), and excellent (UPF ≥ 40). In this study, cotton, Cl–PSPH–PHDTMS/cotton and Cl–PSPH–ZnO–PHDTMS/cotton were cut into 50 × 50 mm^2 and tested by a UV protective factor tester (CARY50, China). Additionally, ventilation property was tested at room temperature using an air permeability tester (YG461E, China) according to GB/T 5453-1997 method. Briefly, each specimen (20 × 20 cm^2) was fixed into the tester by using 100 Pa air pressure through the fabric, then the rate of air flow was recorded for air permeability analysis.

Antibacterial test

S. aureus (ATCC 6538) and *E. coli* O157:H7 (ATCC 43895) strains were incubated overnight at 37 °C in Luria–Bertani broth, harvested by centrifugation, and washed twice with phosphate-buffered saline (PBS). An aliquot of 25 µL bacterial solution was dripped onto the center of a one inch square swatch and covered with another identical swatch which was held in place by a sterile weight. When the contact times reached 5 min, 10 min, and 30 min, each sample was quenched with 5 mL sodium thiosulfate solution (0.02 N) to remove oxidative chlorines. Then, a ten-fold serial dilution was used to prepare bacterial suspensions and each dilution was spread on agar plates. Then, the plates were incubated at 37 °C for 24 h, and the bacterial colonies were recorded for biocidal efficacy analysis.

In vitro cytotoxicity test

The XTT cytotoxicity test of ZnO NPs and Cl–PSPS–ZnO–PHDTMS/cotton was evaluated using mouse fibroblasts L-929 (ATCC CCL-1) according to ISO 10993-5. Cells were cultured and passaged three times in DMEM (with 10% FBS and 1% antibiotics) at 37 °C in a humid atmosphere with 5% gaseous CO_2. Following that, cells were trypsinized and resuspended in culture medium. An aliquot of 100 µL of the cell suspension (6300 cell/well) was seeded in 96-well plates for another 24 h incubation. Then 100 µL of sample extracts was used to replace the culture medium. After another 24 h incubation, the absorbance of each well at 490 nm was measured with a reference wavelength of 690 nm using a microplate reader. Cells on the culture plate without treatment were served as controls. All the experiments were performed in triplicate.

Results and discussion

Chemical structure and morphologies characterization of the modified cotton

The FT-IR spectra of prepared samples are shown in Fig. 1a. The band at 3367 cm^{-1} was due to the stretching vibrations of –OH mode (spectrum A), and similar bands were observed for the modified samples. The bands in the range of 2904 cm^{-1} and 1369 cm^{-1} were attributed to characteristic C–H stretching and bending vibrations, respectively (Yu et al. 2013). Meanwhile, the absorption bands at 1640 cm^{-1} were ascribed to the C=O stretching in cotton (Navik et al. 2017). A band at 1709 cm^{-1} was found in PSPH–ZnO–PHDTMS/cotton reflecting the successful deposition of PSPH onto cotton substrates (Fei et al. 2018; Pan et al. 2018), which shifted to 1713 cm^{-1} after chlorination, mainly caused by the electron withdrawing effect of oxidative chlorine(Dong et al. 2017). The bands at around 960 cm^{-1} and 1100 cm^{-1} were expected to be the stretching vibration of Si–O–Zn and symmetric stretching of Si–O–C group and were not observed due to the overlap of the strong bands ranging from 900 to 1150 cm^{-1}, attributed to the complex stretching of C–O–C groups (de Oliveira et al. 2016).

To further investigate the chemical composition as well as the binding state of Cl–PSPH–ZnO–PHDTMS/cotton, XPS spectra were investigated (Fig. 1b). In the Fig. 1b (A), two peaks of 286.8 and 580.4 eV were observed in the pristine cotton fabric, which were associated with C 1 s and O 1 s, respectively. Figure 1b (B) shows the stack views of the XPS core patterns of Zn (2p), N (1 s), and Si (2p) on the cotton coated with PSPH–ZnO–PHDTMS. The typical Si 2p region was divided into three peaks, which were 103.00 eV, 102.29 eV, and 101.75 eV. The binding energies at 103–104 eV and 101–102 eV were contributed to the chemical species of Si–O–Si and Si–O–C, respectively (Bastarrachea and Goddard 2013). The peak at 102.29 eV was related to the chemical species of Si–O–Zn (Jeong et al. 2014) (Fig. 1c). The obtained data can be explained by the attachment modes between siloxane molecules and the matrix surface. In addition to the formation of Si–O–Si bonds between adjacent siloxane molecules, the surface complexes occurred through dehydration of Si–OH with the hydroxyl groups of cotton and ZnO reported previously (Kamegawa et al. 2012; Mallakpour and Nikkhoo 2013). After chlorination, an additional peak with binding energy of 200 eV appeared (Fig. 1 d) reflecting that the N–H groups were converted into N–Cl covalent bonds(Ma et al. 2016).

The SEM photographs of cotton, PSPH–ZnO–PHDTMS/cotton, and Cl–PSPH–ZnO–PHDTMS/cotton were presented in Fig. 2 (a, b, c). A smooth surface

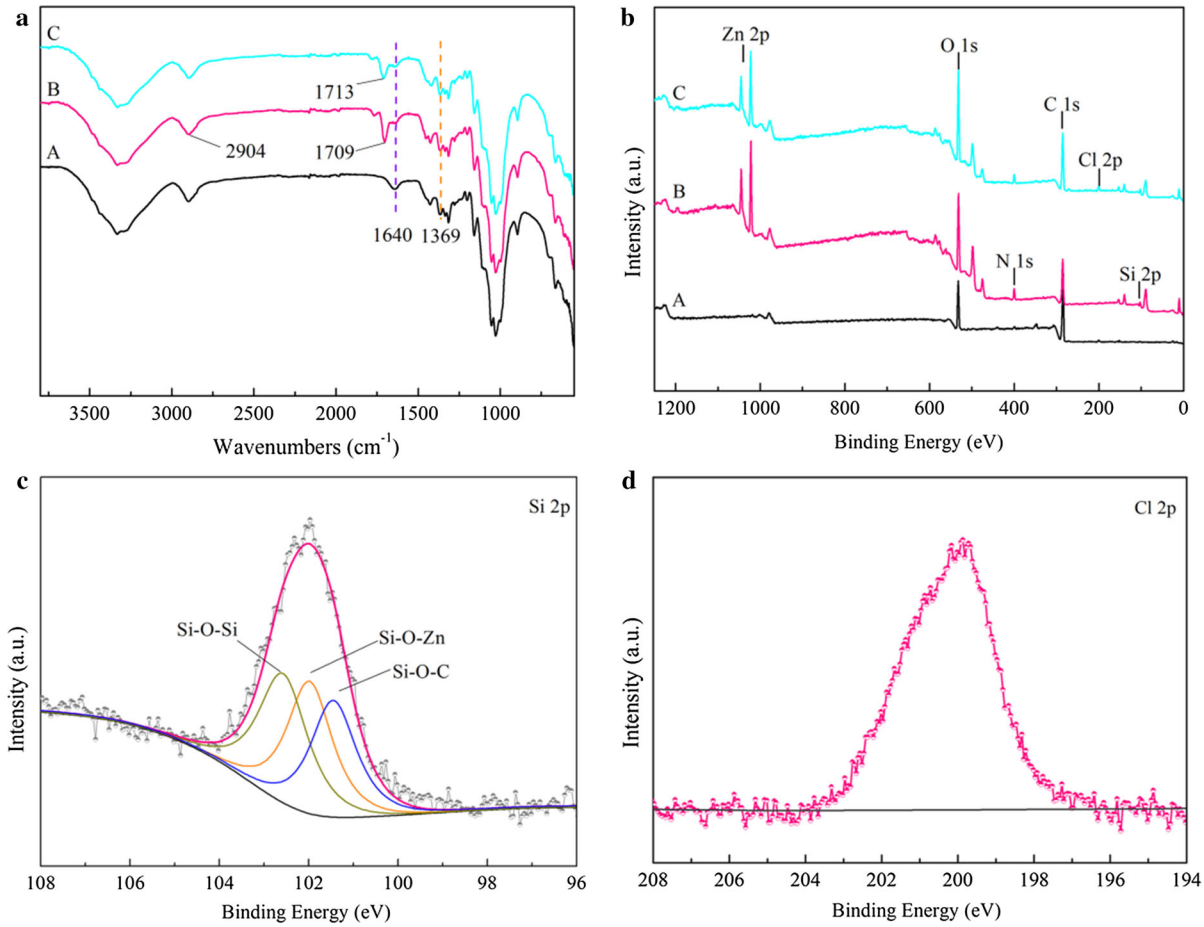

Fig. 1 FT-IR (**a**) and XPS spectra of cotton before and after modification (**b**) (cotton (A) PSPH–ZnO–PHDTMS/cotton (B) and Cl–PSPH–ZnO–PHDTMS/cotton (C)) Si 2p (**c**) and Cl 2p of Cl–PSPH–ZnO–PHDTMS/cotton (**d**)

was observed for untreated cotton. Once modified with siloxane and ZnO particles, Cl–PSPH–ZnO–PHDTMS/cotton showed rough surface with dispersed particles, which indicated the coating of the hybrid composites on cotton was successful. Figure 2d showed the XRD patterns of cotton and Cl–PSPH–ZnO–PHDTMS/cotton. It can be seen that three sharp diffraction peaks occurred in Cl–PSPH–ZnO–PHDTMS/cotton samples, at 31.7°, 34.4°, 36.2°, which were indexed to the wurtzite structure of ZnO (Kadam et al. 2018). The intense and sharp peaks elucidated that the products were well-crystallized.

Chlorine content and hydrophobic stability towards washing

The stability of Cl–PSPH–ZnO–PHDTMS/cotton with initial chlorine load of (0.33 ± 0.05)% was studied. The chlorine content gradually decreased with the increase of washing cycles due to the hydrolysis of N–Cl bonds and amide group. After 25 washing cycles, the chlorine load decreased to (0.23 ± 0.02)%, which was still effective in inactivating bacteria. Meanwhile, most of the chlorine could be regained upon exposure to household bleach solution, indicating a full recovery of the biocidal efficacy.

The water contact angles of Cl–PSPH–ZnO–PHDTMS/cotton were also investigated against different laundering cycles. The surface of Cl–PSPH–ZnO–PHDTMS/cotton exhibited good hydrophobicity

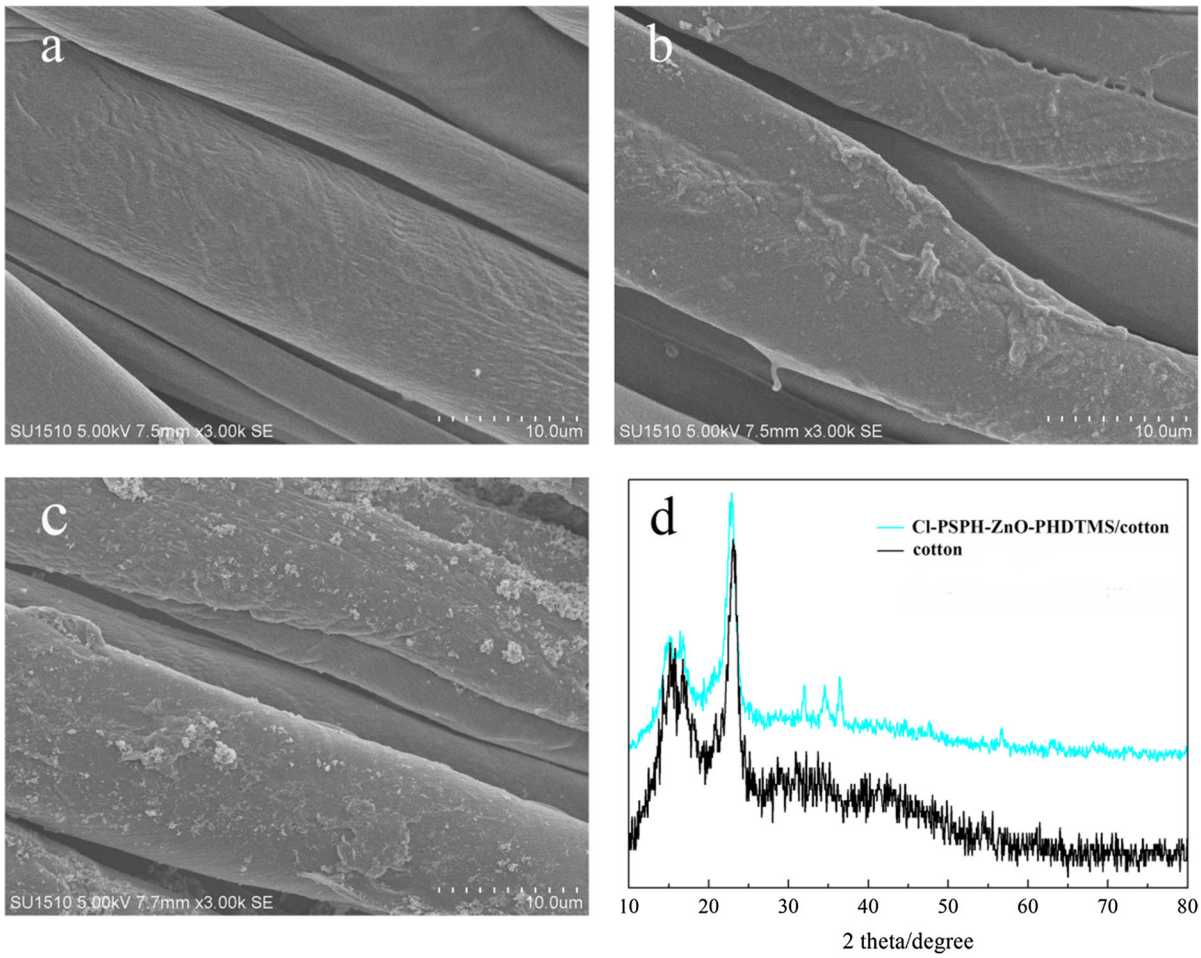

Fig. 2 The SEM images of cotton (**a**) PSPH–ZnO–PHDTMS/cotton (**b**) and Cl–PSPH–ZnO–PHDTMS/cotton (**c**) XRD spectra of cotton and Cl–PSPH–ZnO–PHDTMS/cotton (**d**)

with a contact angle of 139° ± 2°. The coated samples had a contact angle of 117° ± 2° after 25 cycles of laundering indicating that the hydrophobic surface was durable for potential long-term application. According to Fig. 3b, sliding angle showed slightly increased from 18° ± 2° to 26° ± 4° after 10 times washing. With the extension to 25 cycles, water droplets required a large angle of 50° ± 2° to roll off the surface of the modified cotton fabrics which was due to the damage of hydrophobic film by washing. Obviously, a stream of water could clean the contamination on the treated fabrics laundered 25 cycles and the surface of the fabric remained dry, which showed favorable self-cleaning capabilities (Fig. 3c). These results showed that the hybrid composites on cotton were quite stable to withstand laundering since the compounds were bonded to cotton via covalent bonding.

Breaking strength

The breaking strengths of chlorinated and unchlorinated swatches in warp and weft directions are presented in Fig. 4. Compared to the control samples, the coating of PSPH–ZnO–PHDTMS on cotton showed a small degree of tensile strength loss. Chlorination process has little effect on the breaking strength of the PSPH–ZnO–PHDTMS coated cotton fabrics, and more than 90% of the original breaking strength was maintained in warp and weft directions

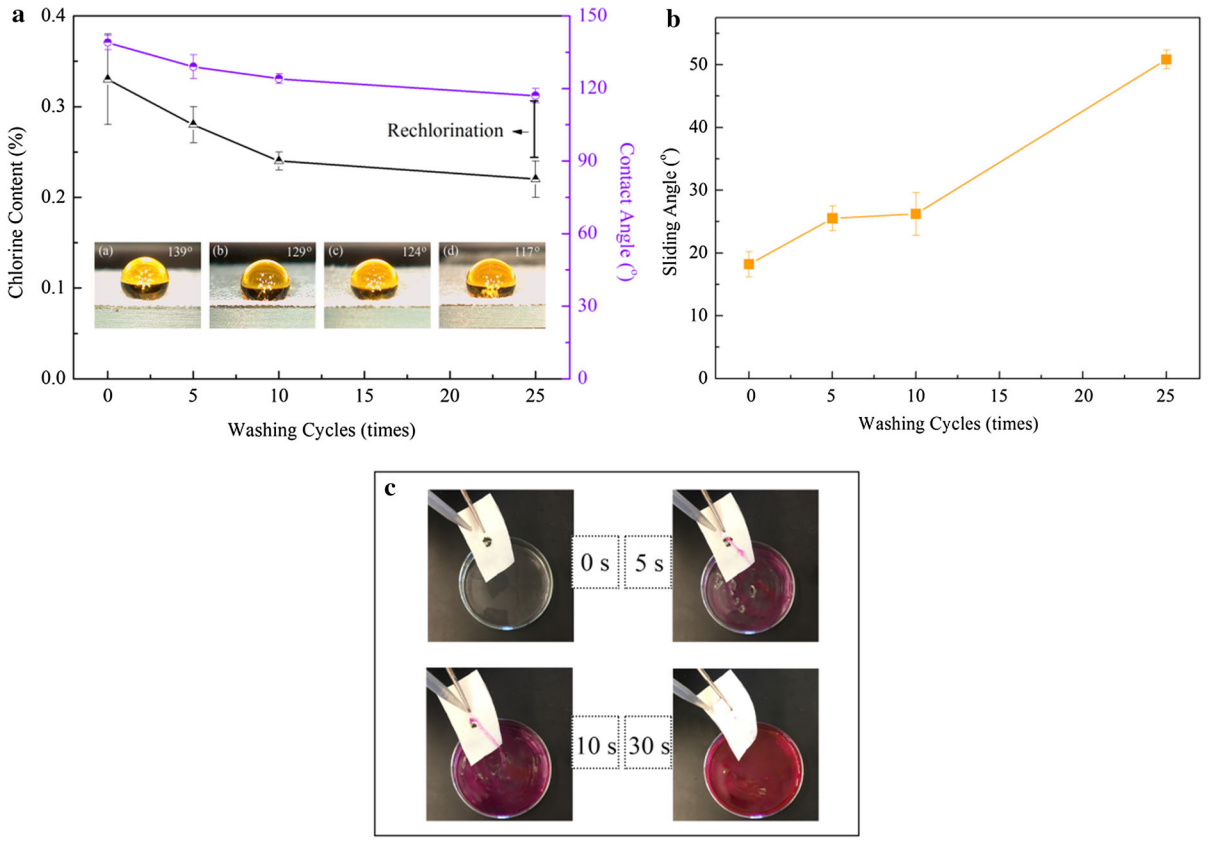

Fig. 3 Chlorine content and contact angle (**a**) sliding angle (**b**) of Cl–PSPH–ZnO–PHDTMS/cotton before and after various washing cycles captured images of water droplet movement at different time periods on the surface of Cl–PSPH–ZnO–PHDTMS/cotton laundered 25 cycles (**c**)

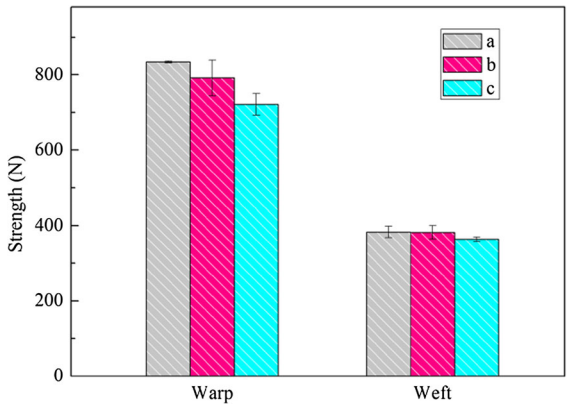

Fig. 4 Tensile strengths of cotton (**a**) PSPH–ZnO–PHDTMS/cotton (**b**) and Cl–PSPH–ZnO–PHDTMS/cotton (**c**)

after chlorination. The results indicated that the addition of PSPH, PHDTMS and ZnO NPs on the fabric did not cause significant damage to fabric structures.

UV light stability and air permeability

Kocer et al. (2010) reported that the scission reaction existing in N-chlorinated coatings could cause unrecovered chlorine loss upon heat and UV irradiation. Li et al. found that the introduction of titanium dioxide could significantly improve the UV stability of N-halamine diol and N-halamine siloxane, respectively (Li et al. 2013; 2014). In this study, ZnO nanoparticles were added into solution with N-halamines to prevent the breaking of the N–Cl bonds. Table 1 showed that the chlorine degradation in Cl–PSPH–PHDTMS/cotton was fast in the initial 4 h of irradiation, and about 71% chlorine was lost. While the Cl–PSPH–ZnO–PHDTMS/cotton had better UV stability, and only about 50% chlorine was lost with same irradiation conditions. After 24 h, almost all the loaded chlorine was lost in Cl–PSPH–PHDTMS/cotton. While Cl–PSPH–ZnO–PHDTMS/cotton retained

Table 1 UV light stability of Cl–PSPH/cotton and Cl–PSPH–ZnO–PHDTMS/cotton

Irradiation time (h)	Chlorine loadings (%)	
	Cl–PSPH–PHDTMS/cotton	Cl–PSPH–ZnO–PHDTMS/cotton
0	0.32 ± 0.02	0.30 ± 0.03
1	0.17 ± 0.04	0.21 ± 0.05
2	0.16 ± 0.02	0.19 ± 0.01
4	0.10 ± 0.01	0.16 ± 0.01
8	0.09 ± 0.03	0.16 ± 0.02
12	0.06 ± 0.01	0.14 ± 0.01
24	0.05 ± 0.01	0.14 ± 0.01
48	0 ± 0	0.14 ± 0.03
72	0 ± 0	0.14 ± 0.02
24 (Rechlorination)	0.16 ± 0.02	0.27 ± 0.02
72 (Rechlorination)	0.15 ± 0.04	0.24 ± 0.01

about 50% of its initial chlorine load. As reported by Li et al. about 80% of the chlorine loadings were regained for the cotton coated with TiO_2 after 24 h of UV irradiation when exposure to sodium hypochlorite solution. Herein, 90% of the active chlorine on Cl–PSPH–ZnO–PHDTMS/cotton could be recovered after 24 h of irradiation. Notably, with the extension to 72 h, it was observed that the chlorine load of Cl–PSPH–ZnO–PHDTMS/cotton was maintained at a constant level, and 83% of the lost chlorine on Cl–PSPH–ZnO–PHDTMS/cotton could be recovered upon the exposure to an aqueous sodium hypochlorite solution compared with 47% recovery of the lost chlorine on Cl–PSPH–PHDTMS/cotton. Overall, ZnO nanoparticles significantly reduce the chlorine loss of hydantoin unities from the surface of the coated cotton and showed remarkable stability towards long-term UV light irradiation.

The effect of ZnO NPs on the UV-protection of the treated fabric was also studied. Table 2 shows that the addition of ZnO in the coatings of cotton fabric could significantly improve UV protection with UPF values increasing from 5.45 to 101.16. Interestingly, the UPF values did not change obviously even after 25 washing cycles. However, Cl–PSPH–PHDTMS coatings without ZnO didn't show any UV-protection capability with UPF value of 5.36. Compared with the cotton control, air permeability of chlorinated PSPH–PHDTMS/cotton decreased slightly, which might be due to the deposition of polymers on the surface of cotton fabrics. After coated with ZnO, the air permeability of Cl–PSPH–ZnO–PHDTMS/cotton decreased from 150.66 mm/s to 113.14 mm/s due to the coverage of ZnO nanoparticles and polymers on the surface of substrates.

Antibacterial and in vitro cytocompatibility evaluations

The biocidal efficacies of the cotton swatches coated with PSPH–PHDTMS and PSPH–ZnO–PHDTMS against *S. aureus* and *E. coli* O157:H7 are shown in Table 3. The control cotton caused a certain degree reduction of bacteria due to the adhesion of the

Table 2 UV-protection property and air permeability of cotton, Cl–PSPH–PHDTMS/cotton and Cl–PSPH–ZnO–PHDTMS/cotton

Sample	UPF	Air permeability (mm/s)
Cotton	5.45 ± 1.77	150.66 ± 0.64
Cl–PSPH–PHDTMS/cotton	5.36 ± 0.41	144.82 ± 0.90
Cl–PSPH–ZnO–PHDTMS/cotton	101.16 ± 24.32	113.14 ± 1.22
Cl–PSPH–ZnO–PHDTMS/cotton[a]	85.82 ± 13.22	–

[a]The modified cotton after 25 cycles of laundering

Table 3 Antibacterial efficacies of the treated cotton against bacteria

Sample	Contact time (min)	Bacterial reduction (%)	
		S.aureus[a]	*E. coli* O157:H7[b]
Cotton	30	78.11	60.80
PSPH–PHDTMS–ZnO/cotton	30	28.53	41.20
Cl–PSPH–PHDTMS/cotton[c]	5	86.60	80.40
	10	99.87	97.33
	30	100	100
Cl–PSPH–ZnO–PHDTMS/cotton[c]	5	99.99	99.99
	10	100	100
	30	100	100

[a]Inoculum was 1.50×10^6 CFU per sample

[b]Inoculum was 3.76×10^6 CFU per sample

[c]The initial cotton concentration was 0.24%

bacteria to the fabrics instead of inactivation (Pan et al. 2018). After coated with PSPH–ZnO–PHDTMS, the samples showed the bacterial reduction rates of 28.53% and 41.20% against *S. aureus* and *E. coli* O157:H7 with 30 min contact, respectively. After chlorination, the Cl–PSPH–PHDTMS/cotton samples inactivated 100% of *S. aureus* and *E. coli* O157:H7 within 30 min. The Cl–PSPH–ZnO–PHDTMS/cotton samples could cause 100% reduction on both bacteria with 10 min contact, which was due to the larger functional surface area of N-halamines with the introduction of ZnO NPs. The N-halamine compounds, high efficient antibacterial agents, can directly contact with the bacterial cell, transfer oxidative halogen (Cl^+) to biological receptor, and then destroy the cell by oxidizing the cells by oxidizing thiol groups or halogenating amino groups in proteins(Lin et al. 2018). The addition of ZnO in the coating with N-halamines could enhance antibacterial efficacy.

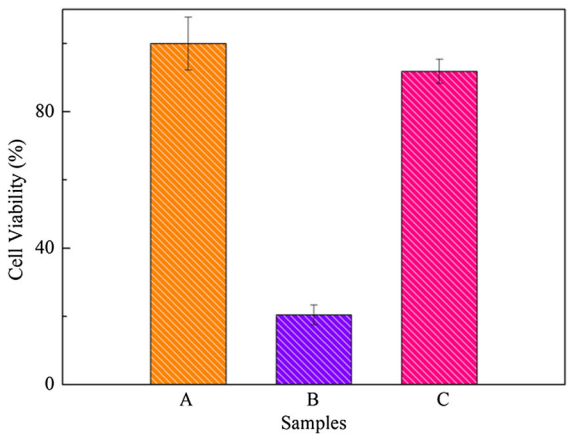

Fig. 5 Cell viability of control (a) ZnO NPs (b) Cl–PSPH–ZnO–PHDTMS/cotton (c) after 24 h incubation

Figure 5 shows the cell viability after exposed to ZnO NPs and Cl–PSPH–ZnO–PHDTMS/cotton hybrid extracts for 24 h. As can be seen, ZnO NPs represented toxic performance, which might be due to the release of Zn^{2+}(Aditya et al., 2019). However, after coating onto fabrics with siloxane, Cl–PSPH–ZnO–PHDTMS/cotton showed good biocompatibility with 91.86% viable cells. These results are consistent with previous findings that silane-modified ZnO nanoparticles could delimit Zn^{2+} ionic dissolution and maintain NPs dispersion, thus improved their safety (Mu et al. 2014; Zabihi et al. 2019).

Conclusion

N-halamine precursor was synthesized and coated onto cotton fabrics with ZnO NPs and silane via a pad-dry-cure process. The characterization of the coated cotton fabrics by FT-IR, SEM, XRD and XPS confirmed the successful coatings of the hybrids. The coated fabrics were rendered antibacterial after exposure to diluted household bleach. The biocompatible Cl–PSPH–ZnO–PHDTMS/cotton samples had excellent antibacterial activities and caused 100% reduction of inoculated *S. aureus* (ATCC 6538) and *E. coli* O157:H7 (ATCC 43895) within 10 min. Hydrophobicity of Cl–PSPH–ZnO–PHDTMS/cotton was quite stable even after 25 washing cycles. The chlorinated Cl–PSPH–ZnO–PHDTMS/cotton samples exhibited prominent UV light stability, and about 83% of the active chlorine could be regained after 72 h of irradiation, which were still effective in killing bacteria. The prepared Cl–PSPH–ZnO–PHTDMS/cotton fabrics have potential for outdoor textiles.

Acknowledgments We acknowledge the support the national first-class discipline program of Light Industry Technology and Engineering (LITE2018-21), the Fundamental Research Funds for the Central Universities (Nos. JUSRP51722B and JUSRP11806), the Project of Jiangsu Science and Technological Innovation Team, and 111 Projects (B17021).

References

Aditya A, Chattopadhyay S, Gupta N, Alam S, Veedu AP, Pal M, Singh A, Santhiya D, Ansari KM, Ganguli M (2019) ZnO nanoparticles modified with an amphipathic peptide show improved photoprotection in skin. ACS Appl Mater Interfaces 11:56–72

Bastarrachea LJ, Goddard JM (2013) Development of antimicrobial stainless steel via surface modification with N-halamines: characterization of surface chemistry and N-halamine chlorination. J Appl Polym Sci 127:821–831

Chen Q, Miyata N, Kokubo T, Nakamura T (2015) Bioactivity and mechanical properties of PDMS-modified CaO–SiO_2–TiO_2 hybrids prepared by sol-gel process. J Biomed Mater Res 51:605–611

de Oliveira RD, Calaça G, Santos C, Fujiwara S, Pessoa C (2016) Preparation, characterization and electrochemistry of Layer-by-Layer films of silver nanoparticles and silsesquioxane polymer. Colloid Surf A 509:638–647

Demir B, Broughton RM, Huang TS, Bozack M, Worley SD (2017) Polymeric antimicrobial N-halamine-surface modification of stainless steel. Ind Eng Chem Res 56:11773–11781

Dong Q, Dong A, Morigen (2015) Evaluation of novel antibacterial N-halamine nanoparticles prodrugs towards susceptibility of *Escherichia coli* induced by DksA protein. Molecules 20:7292–7308

Dong A, Huang Z, Lan S, Wang Q, Bao S, Siriguleng, Zhang Y, Gao G, Liu F, Harnoode C (2014) N-halamine-decorated polystyrene nanoparticles based on 5-allylbarbituric acid: from controllable fabrication to bactericidal evaluation. J Colloid Interface Sci 413:92–99

Dong X, Feng L, Ning Z, Xiao F, Wang J, Tan Y (2016) CO2 hydrogenation to methanol over Cu/ZnO/ZrO_2 catalysts prepared by precipitation-reduction method. Appl Catal B Environ 191:8–17

Dong A, Wang Y-J, Gao Y, Gao T, Gao G (2017) Chemical insights into antibacterial N-halamines. Chem Rev 117:4806–4862

Fei Z, Liu B, Zhu M, Wang W, Yu D (2018) Antibacterial finishing of cotton fabrics based on thiol-maleimide click chemistry. Cellulose 25:3179–3188

Horsthuis WHG (2017) ZnO processing for integrated optic sensors. Thin Solid Films 137:185–192

Jang J, Kim Y (2008) Fabrication of monodisperse silica-polymer core-shell nanoparticles with excellent antimicrobial efficacy. Chem Commun 34:4016–4018

Jeong K-S, Oh S-K, Shin H-S, Yun H-J, Kim S-H, Lee H-R, Han K-M, Park H-Y, Lee H-D, Lee G-W (2014) Novel silicon surface passivation by Al_2O_3/ZnO/Al_2O_3films deposited by thermal atomic layer deposition. Jpn J Appl Phys 53:04ER191–04ER195

Jeong D, Kim HK, Jeong JP, Dindulkar SD, Cho E, Yang YH, Jung S (2016) Cyclosophoraose/cellulose hydrogels as an efficient delivery system for galangin, a hydrophobic antibacterial drug. Cellulose 23:1–17

Jin G, Qin H, Cao H, Qian S, Zhao Y, Peng X, Zhang X, Liu X, Chu PK (2014) Synergistic effects of dual Zn/Ag ion implantation in osteogenic activity and antibacterial ability of titanium. Biomaterials 35:7699–7713

Kadam AN, Bhopate DP, Kondalkar VV, Majhi SM, Bathula CD, Tran A-V, Lee S-W (2018) Facile synthesis of Ag–ZnO core–shell nanostructures with enhanced photocatalytic activity. J Ind Eng Chem 61:78–86

Kamegawa T, Seto H, Matsuura S, Yamashita H (2012) Preparation of hydroxynaphthalene-modified TiO_2 via formation of surface complexes and their applications in the photocatalytic reduction of nitrobenzene under visible-light irradiation. ACS Appl Mater Interfaces 4(12):6635–6639

Kocer HB, Akdag A, Worley SD, Acevedo O, Broughton RM, Wu Y (2010) Mechanism of photolytic decomposition of N-halamine antimicrobial siloxane coatings. ACS Appl Mater Interfaces 42:2456–2464

Li J, Li R, Du J, Ren X, Worley SD, Huang TS (2013) Improved UV stability of antibacterial coatings with N-halamine/TiO_2. Cellulose 20:2151–2161

Li J, Liu Y, Jiang Z, Ma K, Ren X, Huang T-S (2014) Antimicrobial cellulose modified with nanotitania and cyclic N-halamine. Ind Eng Chem Res 53:13058–13064

Lin X, Yin M, Liu Y, Li L, Ren X, Sun Y, Huang T (2018) Biodegradable polyhydroxybutyrate/poly-ε-caprolactone fibrous membranes modified by silica composite hydrol for super hydrophobic and outstanding antibacterial application. J Ind Eng Chem 63:303–311

Ma W, Li J, Liu Y, Ren X, Gu Z-G, Xie Z, Liang J (2016) Preparation and characterization of excellent antibacterial TiO_2/N-halamines nanoparticles. Colloid Surf A 506:284–290

Mallakpour S, Nikkhoo E (2013) Production and characterization of nanocomposites based on poly(amide-imide) containing 4,4′-methylenebis(3-chloro-2,6-diethylaniline) using nano-TiO_2 surface-coupled by 3-aminopropyltriethoxysilane. Prog Org Coat 76:231–237

Mu Q, David CA, Galceran J, Rey-Castro C, Krzemiński Ł, Wallace R, Bamiduro F, Milne SJ, Hondow NS, Brydson R et al (2014) Systematic investigation of the physicochemical factors that contribute to the toxicity of ZnO nanoparticles. Chem Res Toxicol 27:558–567

Navik R, Thirugnanasampanthan L, Venkatesan H, Kamruzzaman M, Shafiq F, Cai Y (2017) Synthesis and application of magnesium peroxide on cotton fabric for antibacterial properties. Cellulose 24:3573–3587

Olson DC, Lee YJ, White MS, Kopidakis N, Shaheen SE, Ginley DS, Voigt JA, Hsu JWP (2015) Effect of ZnO processing on the photovoltage of ZnO/Poly(3-hexylthiophene) solar cells. J Phys Chem C 112:9544–9547

Pan N, Liu Y, Ren X, Huang T-S (2018) Fabrication of cotton fabrics through in situ reduction of polymeric N-halamine modified graphene oxide with enhanced ultraviolet-blocking, self-cleaning, and highly efficient, and monitorable antibacterial properties. Colloid Surf A 555:765–771

Shahidi S, Rezaee H, Rashidi A, Ghoranneviss M (2017) In situ synthesis of ZnO Nanoparticles on plasma treated cotton fabric utilizing durable antibacterial activity. J Nat Fibers 15:1–9

Silva LFD, M'Peko JC, Catto AC, Bernardini S, Mastelaro VR, Aguir K, Ribeiro C, Longo E (2017) UV-enhanced ozone gas sensing response of ZnO–SnO_2 heterojunctions at room temperature. Sens Actuators B-Chem 240:573–579

Worley SD, Chen Y, Wang JW, Wu R, Cho U, Broughton RM, Kim J, Wei CI, Williams JF, Chen J et al (2005) Novel N-halamine siloxane monomers and polymers for preparing biocidal coatings. Surf Coat Int Part B Coat Trans 88:93–99

Xu Q, Xie L, Diao H, Li F, Zhang Y, Fu F, Liu X (2017) Antibacterial cotton fabric with enhanced durability prepared using silver nanoparticles and carboxymethyl chitosan. Carbohydr Polym 177:187–193

Yazhini KB, Prabu HG (2015) Antibacterial activity of cotton coated with ZnO and ZnO–CNT composites. Appl Biochem Biotech 175:85–92

Yu H, Zhang X, Zhang Y, Liu J, Zhang H (2013) Development of a hydrophilic PES ultrafiltration membrane containing SiO_2@N-Halamine nanoparticles with both organic antifouling and antibacterial properties. Desalination 326:69–76

Zabihi E, Babaei A, Shahrampour D, Arab Z, Mirshahidi K, Joz Majidi H (2019) Facile and rapid in situ synthesis of chitosan-ZnO nano-hybrids applicable in medical purposes; a novel combination of biomineralization, ultrasound, and bio-safe morphology-conducting agent. Int J Biol Macromol 131:107–116

Zhang J, Sun L, Yin J, Su H, Chunsheng Liao A, Yan C (2016a) Control of ZnO morphology via a simple solution route. Chem Mater 14:4172–4177

Zhang L, Zhang L, Yang Y, Zhang W, Lv H, Yang F, Lin C, Tang P (2016b) Inhibitory effect of super-hydrophobicity on silver release and antibacterial properties of super-hydrophobic Ag/TiO_2 nanotubes. J Biomed Mater Res B 104:1004–1012

Zhao L, Yan X, Jie Z, Yang H, Yang S, Liang J (2014) Regenerable antimicrobial N -halamine/silica hybrid nanoparticles. J Biomed Mater Res B 16:1–12